Letter

optica

Uniqueness in multi-spectral constant-wave epi-illumination imaging

P. BEATRIZ GARCIA-ALLENDE,[1,*] KARIN RADRICH,[1] PANAGIOTIS SYMVOULIDIS,[1] JÜRGEN GLATZ,[1] MAXIMILIAN KOCH,[1] KARIN M. JENTOFT,[1] JORGE RIPOLL,[2] AND VASILIS NZIACHRISTOS[1,*]

[1]*Chair for Biological Imaging & Institute for Biological and Medical Imaging, Technische Universität München and Helmholtz Zentrum München, Trogerstr. 9 D-81675, München, Germany*

[2] *Dept. of Bioengineering and Aerospace Engineering, University Carlos III of Madrid, Avda. de la Universidad 30, 28911 Madrid, Spain*

**Corresponding author: v.ntziachristos@tum.de; pbgarciaallende@gmail.com*

Received XX Month XXXX; revised XX Month, XXXX; accepted XX Month XXXX; posted XX Month XXXX (Doc. ID XXXXX); published XX Month XXXX

Multispectral tissue imaging based on optical cameras and continuous-wave tissue illumination is commonly used in medicine and biology. However, an in-depth understanding of the quantitative ability of these spectral measurements is needed before concluding on their diagnostic or theranostic ability. Surprisingly, there is a characteristic absence of a critical look at the quantities that can be uniquely characterized from optically diffuse matter by multispectral imaging. We investigate here the fundamental question of uniqueness in epi-illumination measurements from turbid media obtained at multiple wavelengths. By utilizing an analytical model, controlled tissue-mimicking phantoms and an in-vivo imaging experiment we show that independently of the bands employed, spectral measurements cannot uniquely retrieve absorption and scattering coefficients. We also establish that it is, nevertheless, possible to uniquely quantify oxygen saturation and the Mie scattering power, a previously undocumented uniqueness condition. © 2015 Optical Society of America

OCIS codes: *(170.0110) Imaging systems, (170.1470) Blood or tissue constituent monitoring, (170.1610) Clinical applications, (170.3660) Light propagation in tissues, (170.3880) Medical and biological imaging.*

http://dx.doi.org/10.1364/optica.99.099999

Epi-illumination tissue imaging using optical cameras is commonly employed in diagnostic and theranostic medicine, for example in surgery, dermatology or endoscopy [1-3]. While conventional color imaging is performed at 3 or 4 spectral bands, imaging and data processing at an increased number of wavelengths, dubbed multi-spectral, has been considered for improving the diagnostic value of these procedures [4]. In dermatology, multispectral epi-illumination imaging (MSEI) has been investigated for melanoma diagnosis [5] or for assessing the burn depth and the healing timeline [6] and in ophthalmology, for detecting retinal diseases and estimating oximetry maps [7]. Likewise, endoscopic narrow band imaging (NBI) utilizes a blue and a green spectral band to highlight subsurface blood vessels, thereby enhancing the diagnostic yield of white-light endoscopy [8].

The larger part of diagnostic optical imaging is based on the qualitative observation of images or empirical data processing schemes. Disease may be detected for example on color deviation from the normal appearance of healthy tissue. Quantification of tissue optical properties is a highly sought-after target for improving the detection ability and elucidating underlying pathophysiological features [9, 10]. In particular, quantification of tissue absorption or scattering changes may lead to improved diagnostics [11]. The majority of optical imaging used in the clinics is based on measurements performed under constant intensity illumination, i.e. continuous-wave (CW) illumination. However, CW measurements are not capable of retrieving tissue absorption and scattering. In particular, it has been hypothesized, but not experimentally shown [3], that the optical intensity reflected from a diffusive surface at a single wavelength, depends on the quotient between the reduced scattering (μ_s') and absorption (μ_a) coefficient at the respective wavelength, a condition referred to as "scale invariance" [3, 12]. While the inability of single wavelength CW epi-illumination measurements to quantify tissue properties is established, the quantification ability of measurements obtained at multiple wavelengths has not yet been analytically demonstrated. To the best of our knowledge, no investigation has examined uniqueness in the context of multispectral measurements. The underlying premise of this interrogation relates to whether the information carried by apparently independent measurements at different wavelengths indeed carries independent information. We therefore addressed the fundamental question on whether there exist tissue parameters that can be uniquely quantified by epi-illumination measurements at multiple wavelengths. The uniqueness question posed relates generally to measurements from turbid media containing chromophores with distinct absorption spectra and in particular to identifying the range of biomedical applications that can be addressed by multispectral epi-illumination imaging in a quantitative manner. This study of uniqueness was initially based on a theoretical analysis, and then confirmed experimentally.

To study the uniqueness achieved by multi-spectral epi-illumination measurements we use an analytical expression describing epi-illumination measurements [13]. We have recently validated [14] this

newly proposed reflectance model that accounts for the exponential decay of the reduced intensity as it enters the diffusive medium and improves on previously established analytical formulae [15] by allowing the inclusion of arbitrary source profiles. Assuming a detector having a numerical aperture of 1, a turbid medium of index of refraction n_0 and plane-wave CW illumination, the light flux detected is given by [13]:

Fehler! Es ist nicht möglich, durch die Bearbeitung von Feldfunktionen Objekte zu erstellen. **(1)**

where $S_0 = \left(1 - R_{air \to n_0}\right) S^{inc}$ is the power per area that enters the diffusive medium (in Watts/cm²). S_0 incorporates the power lost due to specular reflections at the interface *(z = 0)* with respect to the total incident power per area S^{inc}; μ_a and μ_s' are, respectively, the absorption and reduced scattering coefficient of the turbid medium; $D(\mu_s', \mu_a) = 1/3(\mu_s' + \beta\mu_a)$ is the absorption-dependent diffusion coefficient, whereby β indicates the D dependence on absorption and typically ranges from 0.2 to 0.5 [16]. Note that this dependence with absorption is non-linear since the factor β is also absorption and scattering dependent. This non-linear dependence of the diffusion coefficient with absorption would, in principle, enable the separation of absorption from scattering in a unique manner. However, as it is subsequently demonstrated, the coefficient β only depends further on the quotient of μ_s' and μ_a, not relaxing thus the non-unique characteristic of wavelength dependent separation of μ_s' and μ_a. Finally, in Eq. (1) the boundary coefficient α accounts for the difference in refractive indices [17] between the two media. Introducing the expression for the diffusion coefficient in Eq. (1) and dividing the numerator and denominator by μ_s', the detected flux becomes:

Fehler! Es ist nicht möglich, durch die Bearbeitung von Feldfunktionen Objekte zu erstellen. **(2)**

where $\bar{\mu} = \mu_s'/\mu_a$. The factor β remains dependent on μ_s' and μ_a and represents the key to finding unique values for both μ_s' and μ_a. One would assume that under certain conditions such as the presence of high absorption, the absorption dependence of the diffusion coefficient would provide a means to reduce the scale invariance of $J_{\det}$. However, in order to analyse the scale invariance of $J_{\det}$ with $\bar{\mu}$, we first need to prove the invariance of β with respect to μ_s' and μ_a. This analysis provides the formal mathematical proof for the scale invariance on $\bar{\mu}$ assumed in [3]. According to Aronson et al. [16] this dependence of β on the optical properties is accounted as:

$$\beta = \frac{1}{3D\mu_a} - \frac{\mu_s'}{\mu_a} = \frac{1}{3\frac{\mu_a^2}{F_n\mu_t^2}} - \frac{\mu_s'}{\mu_a} = \frac{1}{3\frac{\mu_a^2}{F_n\left(\mu_a + \frac{\mu_s'}{1-g}\right)^2}} - \frac{\mu_s'}{\mu_a}$$

$$= \frac{F_n\left(\mu_a + \frac{\mu_s'}{1-g}\right)^2}{3} - \frac{\mu_s'}{\mu_a} = \frac{1}{3}F_n\left(1 + \frac{\bar{\mu}}{1-g}\right)^2 - \bar{\mu}$$

$$F_n = h_0 h_1 \left(1 - \frac{4h_0}{h_2} + \left(\frac{4h_0}{h_2}\right)^2 \left(1 - \frac{9}{4}\frac{h_1}{h_3}\right) \left(\frac{4h_0}{h_2}\right)^3 \cdot \left(1 - \frac{27}{4}\frac{h_1}{h_3} + \frac{81}{16}\frac{h_1^2}{16h_3^2} + 9\frac{h_1^2}{h_3^2}\frac{h_2}{h_4} + \cdots\right)\right) \quad (3)$$

where $h_l = (2l+1)\left(1 - \omega g^l\right)$. Since $\omega = \mu_s/\mu_t$, it is possible to rewrite each term in Eq. (3) in terms of the quotient between the reduced scattering coefficient and the absorption coefficient ($\bar{\mu}$) and the anisotropy parameter (g):

$$h_l = (2l+1)\left(1 - \frac{\bar{\mu}}{1-g+\bar{\mu}} g^l\right) \quad (4)$$

Eq. (4) demonstrates that in spite of including the coefficient β in the analysis, the scale invariance on $\bar{\mu}$ holds for the single wavelength case since $\beta(\mu_s', \mu_a) = \beta(\bar{\mu})$. Figure 1 plots the reflectance or the light flux normalized to the incident flux S_0 as a function of $\bar{\mu}$, where it can be seen that $J_{\det}/S_0$ is an injective function, i.e. it monotonically increases with $\bar{\mu}$ and its derivative is always positive and distinct from zero. Therefore, one and only one value of the reflectance corresponds to one value of the quotient between the reduced scattering and the absorption coefficient, and the reflectance function is invertible for $\bar{\mu}$.

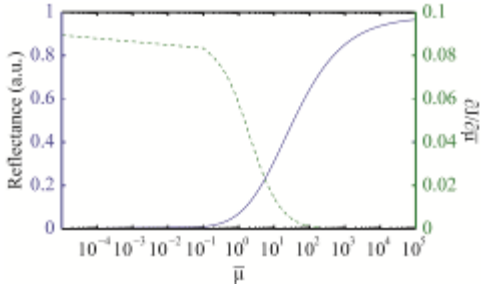

Fig. 1. Dependence of the reflectance (solid line) and the derivative of the reflectance (dotted line) on the quotient of the reduced scattering and absorption coefficient ($\bar{\mu}$).

Assuming blood is the sole absorber present, and without loss of generality, we may now introduce in the expression for $\bar{\mu}$ the spectral properties of the tissue chromophores and the Mie scattering factors:

$$\mu_a(\lambda) = c_{blood}\left(StO_2\,\mu_a^{HbO_2}(\lambda) + (1 - StO_2)\,\mu_a^{Hb}(\lambda)\right) \quad (5)$$

$$\mu_s'(\lambda) = A\lambda^{-b} \quad (6)$$

where c_{blood} corresponds to the blood volume fraction, which is assumed to be the sole absorber, StO_2 is the oxygen saturation, $\mu_a^{HbO_2}(\lambda)$ and $\mu_a^{Hb}(\lambda)$ are respectively the absorption coefficients of oxygenated and de-oxygenated blood, and A and b are the scattering amplitude and the scattering power of the power law dependence on wavelength used to describe the Mie scattering spectrum. Making use of this relationship, the oxygen saturation and the scattering power can be extracted from at least three multispectral measurements. On the

other hand it is not possible to decouple the scattering amplitude and the absolute blood concentration:

$$\bar{\mu}(\lambda) = \frac{\mu_s'(\lambda)}{\mu_a(\lambda)} = \frac{A\lambda^{-b}}{c_{blood}\left(StO_2\mu_a^{HbO_2}(\lambda) + (1-StO_2)\mu_a^{Hb}(\lambda)\right)} \quad (7)$$

which implies that given a semi-infinite homogenous turbid medium with specific blood concentration c_{blood_1} and scattering amplitude A_1, the normalized diffuse reflectance for every wavelength from any other general turbid medium with the same oxygen saturation and scattering power, but matching the conditions $c_{blood_2}/c_{blood_1} = A_2/A_1$ will be identical. This coupling of the absolute optical properties results from the extension of the "scale invariance" condition stated above for a single wavelength to the multispectral case.

In order to confirm the theoretical predictions of Eq. (2) and (7) we then performed two experiments. First, a simple controlled experiment on homogeneous liquid phantoms of known optical properties was carried out to estimate the overall accuracy of the formulae in predicting the oxygen saturation, the scattering power and the ratio between the blood concentration and the scattering amplitude. Then a more realistic experiment recovering these parameters in an in-vivo imaging scenario on a murine model was performed. Phantoms were composed of Intralipid to mimic scattering and blood diluted in NaCl. Intralipid concentration varied from 0.4% to 2%, the corresponding reduced scattering coefficients being computed with the formulation from Michels et al. [18]. Blood concentration varied between 2%, 4% and 6%. Saturation levels covered the 0-100% range, and were obtained adding different amounts of sodium hydrosulfite (Sigma-Aldrich, USA) [19]. A blood gas analyzer was employed to measure the ground truth values. The experimental set-up employed has been described elsewhere [14]. A ~2cm x 2cm region-of-interest from each spectral image was selected and divided into 40 x 40 elements of 25mm² area and the mean values per element and wavelength were computed. System calibration was obtained by measuring the spectral reflectance from a phantom containing only 0.5% Intralipid that was used to normalize all other spectral reflectance curves. Normalized curves were fitted to Eq. (2) according to a least-squares-fitting procedure to extract the relevant parameters, being the upper and lower bounds for the optimization fixed to their physiological ranges [20]. The anisotropy parameter *g* was assumed constant over wavelength and equal to 0.8. Retrieved reduced scattering coefficients were expressed in terms of their relative value with respect to the scattering coefficient of Intralipid 1% at 600 nm [18]. The recovered parameters presented a strong correlation with their true values, reinforcing the accuracy of Eqs. (2) and (7). The adjusted $R^2 > 0.95$ for c_{blood}/A and > 0.98 for the oxygenation level, and the root-mean-square errors 0.041% and 2.1%, respectively. The estimated scattering power varied within the range $\bar{b} \pm \sigma_b = 1.24 \pm 0.17$ for all test phantoms, which is in good agreement with the assumed scattering power ($b = 1.32$) derived from Michels et al. [18].

To further confirm Eq.7 on in-vivo tissue measurements, we imaged the exposed abdomen of an anaesthetized CD1 mouse under regular and 100% O_2 inhalation. The mouse was then sacrificed under anaesthesia. All procedures were approved by the District Government of Upper Bavaria. Motion correction between consecutive images was performed using the Speeded-Up Robust Features (SURF) algorithm [21]. The in-vivo spectra were corrected on a per pixel basis using a measurement from a Spectralon block (Ocean Optics, WS1 Reflectance Standard), employed herein as the reflectance standard. Normalized spectra were then fitted to Eq. 7. The results of these measurements are shown in Fig. 2. Color images composed from the multispectral images are shown in the left column, while the subsequent columns depict the corresponding images of oxygen saturation, the ratio between the absolute blood concentration and the scattering concentration, and the scattering power. As highlighted in the bottom graph, the oxygenation values changed dynamically in direct relationship to the air mixture inhaled by the mouse and eventually decreased when reaching post-mortem. The absolute values, however, differ significantly among organs. These differences in the computed absolute values have also been observed in oxygenation measurements based on alternative approaches [22]. As expected, the maps of c_{blood}/A and the scattering power barely changed during the variations in the oxygen saturation values and provide delineation of the different organs. Estimated values of the parameters for the imaged organs are shown in Table I. The estimated value of the scattering power for the stomach is in particular good agreement with the values reported in the available literature [20], while those of kidney and bowel differ more significantly.

TABLE I. Estimated values of c_{blood}/A and *b* of the imaged organs

Organ	**Fehler! Es ist nicht möglich, durch die Bearbeitung von Feldfunktionen Objekte zu erstellen.**	b
Intestine	0.0307±0.0041	3.43±0.26
Pancreas	0.0100±0.0090	2.16± 0.28
Stomach	0.0156±0.0021	0.81±0.51
Kidney	0.0392±0.0017	1.07±0.26

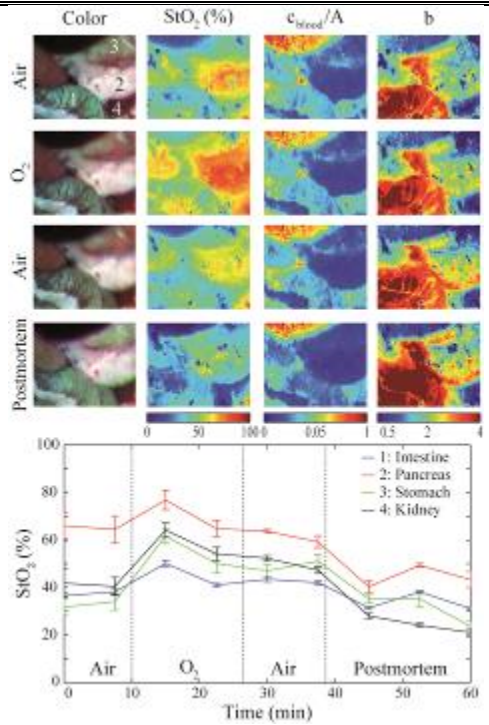

Fig. 2. Emulation of an intraoperative environment in a CD1 mouse. Left images: Color images before turning on the oxygen flow, when breathing 100% O_2, normal air again and, finally, after the mouse was euthanized. The corresponding oxygen saturation, c_{blood}/A and scattering power images are displayed in the second to fourth columns. Bottom graph: Averaged oxygen saturation and standard deviations obtained over regions of interest per organ over time.

In this letter, we analytically and experimentally demonstrated that multispectral measurements of the total diffuse reflectance under constant illumination are scale-invariant with respect to the quotient between absolute values of scattering and blood concentration and, therefore, an infinite set of these values yield identical measurements. To circumvent this limitation, several alternatives have been considered. For oxygen saturation quantification, tissue scattering is commonly assumed to be spatially uniform and known *a priori* [4] or constant with wavelength [23]. These assumptions may lead to

significant errors in calculating oxygen saturation maps [24]. To minimize these errors, the differential pathlength method [25] has also been suggested [24]. The wavelength dependence of the mean path length in tissue is estimated using mostly Monte Carlo simulations, and then the changes in the chromophore concentrations are computed using a modified Beer-Lambert law that incorporates this variable transport path length [26]. The determination of scattering and absorption without the need for assumptions is typically performed by multiple measurements of light intensity at different distances away from a point illumination source [3], however such approach is not applicable to wide-field camera-based imaging, requiring plane-wave illumination. Alternatively, the use of pulsed- [27], or intensity-modulated light [28], or projection of patterns at multiple spatial frequencies [29] has been suggested. These alternative imaging methods gather additional information to measure scattering concurrently with absorption, but at the expense of system cost and complexity. More importantly, none of the previous studies established a relationship between uniqueness and spectral measurements. We established herein that, for the determination of tissue oxygenation, it is not necessary to employ more costly and complex alternatives, thus avoiding pitfalls stemming from partial cross-talk amongst optical parameters [30]. Instead, the determination of tissue oxygenation can be based on CW, plane-illumination measurements without making *a priori* assumptions on the scattering tissue properties. In addition, multispectral measurements may also be used to compute the power law dependence on wavelength, which describes the Mie scattering spectrum and provides tissue morphology information at the microscopic level.

The proposed methodology has been demonstrated in liquid tissue-mimicking phantoms, where strong correlation with the expected values was obtained. The accuracy in oxygen saturation estimations does not longer depend on correct scattering assumptions [23] because scattering parameters are also determined in the process. Moreover, it matches the quantitative performance of wide-field oxygenation imaging using spatially modulated imaging (estimated oxygen saturation values within 5% of the expected values [22]) but avoiding additional system complexity. In a preliminary tissue imaging study, the overall tendency in the oxygen saturation values follows the expectations, while the estimated maps of the ratio between the absolute blood concentration and the scattering amplitude and the scattering power remained notably constant and provide delineation of the different organs. These results demonstrate qualitatively the accuracy of the method, but its quantitative validation is subject to further studies including independent measures of the oxygenation values through a different modality. Also it is yet to be established the ability of the recovered scattering power maps beyond organ differentiation, such whether they provide distinction between tissue types and/or pathological states as those extracted from local reflectance measures. Future research should also focus on the determination of the optimal wavelengths that minimize the error in the parameter estimation while accelerating the acquisition, as well as study the implications that the non-uniqueness of the reflectance has for fluorescence correction approaches based on reflectance ratios.

The research leading to these results has received funding by the Deutsche Forschungsgemeinschaft (DFG), Sonderforschungsbereich-824 (SFB-824), subproject A1 and by the Bundesministerium für Bildung und Forschung (BMBF), grant no. 0315505A (SysTec-Verbund New Methods in Systems Biology "Imaging"). JR acknowledges support from EC FP7 CIG grant HIGH-THROUGHPUT TOMO, and Spanish MINECO grant FIS2013-41802-R.

REFERENCES

1. M. G. Kozberg, B. R. Chen, S. E. DeLeo, M. B. Bouchard, and E. M. Hillman, Proc. Natl Acad. Scie. USA. **110**, 4380 (2013)..
2. B. P. Joshi, S. J. Miller, C. M. Lee, E. J. Seibel, and T. D. Wang, Gastroenterology **143**, 1435 (2012)..
3. G. Zonios, and A. Dimou, Opt. Express **14**, 8661 (2006).
4. N. J. Crane, P. A. Pinto, D. Hale, F. A. Gage, D. Tadaki, A. D. Kirk, I. W. Levin, and E. A. Elster, BMC Surg. **8**, 8 (2008).
5. S. Tomatis, M. Carrara, A. Bono, C. Bartoli, M. Lualdi, G. Tragni, A. Colombo, and R. Marchesini, Phys. Med. Biol. **50**, 1675 (2005).
6. M. A. Afromowitz, J. B. Callis, D. M. Heimbach, L. A. DeSoto, and M. K. Norton, IEEE Trans. Biomed Eng. **35**, 842 (1988).
7. D. Mordant, I. Al-Abboud, G. Muyo, A. Gorman, A. Sallam, P. Ritchie, A. Harvey, and A. McNaught, Eye (Lond). **25**, 309 (2011).
8. L. M. Song, D. G. Adler, J. D. Conway, D. L. Diehl, F. A. Farraye, S. V. Kantsevoy, R. Kwon, P. Mamula, B. Rodriguez, R. J. Shah, and W. M. Tierney, Gastrointest. Endosc. **67**, 581 (2008).
9. V. Krishnaswamy, P. J. Hoopes, K. S. Samkoe, J. A. O'Hara, T. Hasan, and B. W. Pogue, " J. Biomed. Opt. **14**, 014004 (2009).
10. D. Hsiang, A. Durkin, J. Butler, B. J. Tromberg, A. Cerussi, and N. Shah, J. Biomed. Opt. **11**, 044005 (2006).
11. A. M. Laughney, V. Krishnaswamy, E. J. Rizzo, M. C. Schwab, R. J. Barth, B. W. Pogue, K. D. Paulsen, and W. A. Wells, Clin. Cancer Res. **18**, 6315 (2012).
12. A. Ishimaru, *Wave propagation and scattering in random media* (Academic press New York, 1978).
13. J. Ripoll, *Principles of diffuse light propagation: Light propagation in tissues with applications in biology and medicine* (World Scientific, 2012).
14. P. Symvoulidis, K. M. Jentoft, P. B. Garcia-Allende, J. Glatz, J. Ripoll, and V. Ntziachristos, Opt. Lett. **39**, 3919 (2014).
15. T. J. Farrell, M. S. Patterson, and B. Wilson, Med. Phys. **19**, 879 (1992).
16. R. Aronson, and N. Corngold, J. Opt. Soc. Am. A Opt. Image Sci. Vis. **16**, 1066 (1999).
17. R. Aronson, J. Opt. Soc. Am. A Opt. Image Sci. Vis. **12**, 2532 (1995).
18. R. Michels, F. Foschum, and A. Kienle, Opt. Express **16**, 5907 (2008).
19. K. Briely-Sabo, and A. Bjornerud, *Proc. Intl. Sot. Mag. Reson. Med* **8**, 2025 (2000).
20. S. L. Jacques, Phys. Med. Biol. **58**, R37 (2013).
21. H. Bay, A. Ess, T. Tuytelaars, and L. Van Gool, Comput. Vis. Image Und. **110**, 346 (2008).
22. S. Gioux, A. Mazhar, B. T. Lee, S. J. Lin, A. M. Tobias, D. J. Cuccia, A. Stockdale, R. Oketokoun, Y. Ashitate, and E. Kelly, J. Biomed. Opt. **16**, 086015 (2011).
23. N. T. Clancy, D. Stoyanov, D. R. James, A. Di Marco, V. Sauvage, J. Clark, G.-Z. Yang, and D. S. Elson, Biomed. Opt. Express **3**, 2567 (2012).
24. M. Kohl, U. Lindauer, G. Royl, M. Kühl, L. Gold, A. Villringer, and U. Dirnagl, Phys. Med. Biol. **45**, 3749 (2000).
25. M. B. Bouchard, B. R. Chen, S. A. Burgess, and E. Hillman, Opt. Express **17**, 15670 (2009).
26. R. Renaud, C. Martin, H. Gurden, and F. Pain, J. Biomed. Opt. **17**, 0160121 (2012).
27. B. Chance, J. S. Leigh, H. Miyake, D. S. Smith, S. Nioka, R. Greenfeld, M. Finander, K. Kaufmann, W. Levy, M. Young, and et al., P. Natl. Acad. Sci. USA **85**, 4971 (1988).
28. M. S. Patterson, J. D. Moulton, B. C. Wilson, K. W. Berndt, and J. R. Lakowicz, Appl. Optics **30**, 4474 (1991).
29. D. J. Cuccia, F. Bevilacqua, A. J. Durkin, F. R. Ayers, and B. J. Tromberg, J. Biomed. Opt. **14**, 024012 (2009).
30. C. D'Andrea, D. Comelli, A. Pifferi, A. Torricelli, G. Valentini, and R. Cubeddu, J. Phys. D Appl. Phys. **36**, 1675 (2003).

REFERENCES

1. M. G. Kozberg, B. R. Chen, S. E. DeLeo, M. B. Bouchard, and E. M. Hillman, "Resolving the transition from negative to positive blood oxygen level-dependent responses in the developing brain," Proceedings of the National Academy of Sciences 110, 4380-4385 (2013).
2. B. P. Joshi, S. J. Miller, C. M. Lee, E. J. Seibel, and T. D. Wang, "Multispectral endoscopic imaging of colorectal dysplasia in vivo," Gastroenterology 143, 1435 (2012).

3. G. Zonios, and A. Dimou, "Modeling diffuse reflectance from semi-infinite turbid media: application to the study of skin optical properties," Optics Express 14, 8661-8674 (2006).
4. N. J. Crane, P. A. Pinto, D. Hale, F. A. Gage, D. Tadaki, A. D. Kirk, I. W. Levin, and E. A. Elster, "Non-invasive monitoring of tissue oxygenation during laparoscopic donor nephrectomy," BMC Surgery 8, 8 (2008).
5. S. Tomatis, M. Carrara, A. Bono, C. Bartoli, M. Lualdi, G. Tragni, A. Colombo, and R. Marchesini, "Automated melanoma detection with a novel multispectral imaging system: results of a prospective study," Physics in Medicine and Biology 50, 1675-1687 (2005).
6. M. A. Afromowitz, J. B. Callis, D. M. Heimbach, L. A. DeSoto, and M. K. Norton, "Multispectral imaging of burn wounds: a new clinical instrument for evaluating burn depth," IEEE Transactions on Biomedical Engineering 35, 842-850 (1988).
7. D. Mordant, I. Al-Abboud, G. Muyo, A. Gorman, A. Sallam, P. Ritchie, A. Harvey, and A. McNaught, "Spectral imaging of the retina," Eye 25, 309-320 (2011).
8. L. M. Song, D. G. Adler, J. D. Conway, D. L. Diehl, F. A. Farraye, S. V. Kantsevoy, R. Kwon, P. Mamula, B. Rodriguez, R. J. Shah, and W. M. Tierney, "Narrow band imaging and multiband imaging," Gastrointestinal Endoscopy 67, 581-589 (2008).
9. V. Krishnaswamy, P. J. Hoopes, K. S. Samkoe, J. A. O'Hara, T. Hasan, and B. W. Pogue, "Quantitative imaging of scattering changes associated with epithelial proliferation, necrosis, and fibrosis in tumors using microsampling reflectance spectroscopy," Journal of Biomedical Optics 14, 014004 (2009).
10. D. Hsiang, A. Durkin, J. Butler, B. J. Tromberg, A. Cerussi, and N. Shah, "In vivo absorption, scattering, and physiologic properties of 58 malignant breast tumors determined by broadband diffuse optical spectroscopy," Journal of Biomedical Optics 11, 044005 (2006).
11. A. M. Laughney, V. Krishnaswamy, E. J. Rizzo, M. C. Schwab, R. J. Barth, B. W. Pogue, K. D. Paulsen, and W. A. Wells, "Scatter spectroscopic imaging distinguishes between breast pathologies in tissues relevant to surgical margin assessment," Clinical Cancer Research 18, 6315-6325 (2012).
12. A. Ishimaru, Wave propagation and scattering in random media (Academic press New York, 1978).
13. J. Ripoll, Principles of diffuse light propagation: Light propagation in tissues with applications in biology and medicine (World Scientific, 2012).
14. P. Symvoulidis, K. M. Jentoft, P. B. Garcia-Allende, J. Glatz, J. Ripoll, and V. Ntziachristos, "Steady-state total diffuse reflectance with an exponential decaying source," Optics Letters 39, 3919-3922 (2014).
15. T. J. Farrell, M. S. Patterson, and B. Wilson, "A diffusion theory model of spatially resolved, steady-state diffuse reflectance for the noninvasive determination of tissue optical properties invivo," Medical Physics 19, 879-888 (1992).
16. R. Aronson, and N. Corngold, "Photon diffusion coefficient in an absorbing medium," Journal of the Optical Society of America A Optics, Image Science and Vision 16, 1066-1071 (1999).
17. R. Aronson, "Boundary conditions for diffusion of light," Journal of the Optical Society of America A Optics, Image Science and Vision 12, 2532-2539 (1995).
18. R. Michels, F. Foschum, and A. Kienle, "Optical properties of fat emulsions," Optics Express 16, 5907-5925 (2008).
19. K. Briely-Sabo, and A. Bjornerud, "Accurate de-oxygenation of ex vivo whole blood using sodium Dithionite," in Proc. Intl. Sot. Mag. Reson. Med 8 2025 (2000).
20. S. L. Jacques, "Optical properties of biological tissues: a review," Physics in medicine and biology 58, R37 (2013).
21. H. Bay, A. Ess, T. Tuytelaars, and L. Van Gool, "Speeded-up robust features (SURF)," Computer Vision and Image Understanding 110, 346-359 (2008).
22. S. Gioux, A. Mazhar, B. T. Lee, S. J. Lin, A. M. Tobias, D. J. Cuccia, A. Stockdale, R. Oketokoun, Y. Ashitate, and E. Kelly, "First-in-human pilot study of a spatial frequency domain oxygenation imaging system," Journal of Biomedical Optics 16, 086015 (2011).
23. N. T. Clancy, D. Stoyanov, D. R. James, A. Di Marco, V. Sauvage, J. Clark, G.-Z. Yang, and D. S. Elson, "Multispectral image alignment using a three channel endoscope in vivo during minimally invasive surgery," Biomedical Optics Express 3, 2567-2578 (2012).
24. M. Kohl, U. Lindauer, G. Royl, M. Kühl, L. Gold, A. Villringer, and U. Dirnagl, "Physical model for the spectroscopic analysis of cortical intrinsic optical signals," Physics in Medicine and Biology 45, 3749-3764 (2000).
25. M. B. Bouchard, B. R. Chen, S. A. Burgess, and E. Hillman, "Ultra-fast multispectral optical imaging of cortical oxygenation, blood flow, and intracellular calcium dynamics," Optics Express 17, 15670-15678 (2009).
26. R. Renaud, C. Martin, H. Gurden, and F. Pain, "Multispectral reflectance imaging of brain activation in rodents: methodological study of the differential path length estimations and first in vivo recordings in the rat olfactory bulb," Journal of Biomedical Optics 17, 0160121 (2012).
27. B. Chance, J. S. Leigh, H. Miyake, D. S. Smith, S. Nioka, R. Greenfeld, M. Finander, K. Kaufmann, W. Levy, M. Young, and et al., "Comparison of time-resolved and -unresolved measurements of deoxyhemoglobin in brain," Proceedings of the National Academy of Sciences of the United States of America 85, 4971-4975 (1988).
28. M. S. Patterson, J. D. Moulton, B. C. Wilson, K. W. Berndt, and J. R. Lakowicz, "Frequency-domain reflectance for the determination of the scattering and absorption properties of tissue," Applied Optics 30, 4474-4476 (1991).
29. D. J. Cuccia, F. Bevilacqua, A. J. Durkin, F. R. Ayers, and B. J. Tromberg, "Quantitation and mapping of tissue optical properties using modulated imaging," Journal of biomedical optics 14, 024012-024012-024013 (2009).
30. C. D'Andrea, D. Comelli, A. Pifferi, A. Torricelli, G. Valentini, and R. Cubeddu, "Time-resolved optical imaging through turbid media using a fast data acquisition system based on a gated CCD camera," Journal of Physics D: Applied Physics 36, 1675-1681 (2003).